ACS APPLIED MATERIALS & INTERFACES

Research Article

www.acsami.org

# Molecularly Engineered Quantum Dots for Visualization of Hydrogen Sulfide

Yehan Yan,[†,‡,∥] Huan Yu,[†,∥] Yajiao Zhang,[†,‡] Kui Zhang,[†] Houjuan Zhu,[†,‡] Tao Yu,[§] Hui Jiang,[§] and Suhua Wang*[,†,‡]

[†]Institute of Intelligent Machines, Chinese Academy of Sciences, Hefei, Anhui 230031, China

[‡]Department of Chemistry, University of Science & Technology of China, Hefei, Anhui 230026, China

[§]State Key Laboratory of NBC Protection for China, Research Institute of NBC Defense, Beijing 102205, China

Supporting Information

**ABSTRACT:** Among various fluorescence nanomaterials, the II–VI semiconductor nanocrystals (usually called quantum dots, QDs) should be very promising in sensing application because of their high quantum yields, capability for surface property manipulation, and unlimited possible chemical reactions. Herein, we present a fluorescence probe for hydrogen sulfide, which was prepared by first encapsulating inorganic cadmium telluride (CdTe) QDs in silica nanospheres, and subsequently engineering the silica surface with functional molecules azidocoumarin-4-acetic acid reactive to hydrogen sulfide. The nanohybrid probe exhibited two fluorescence bands centered at 452 and 657 nm, respectively. The red fluorescence at 657 nm of the nanohybrid probe is stable against $H_2S$, while the blue fluorescence is specifically sensitive to $H_2S$. The probe showed a distinct fluorescence color evolution from light magenta to blue upon exposure to different amounts of $H_2S$, and a detection limit of 7.0 nM was estimated in aqueous solution. We further applied the nanohybrid probe for visual detection of gaseous $H_2S$ with a low concentration of 0.5 ppm using glass indicating spots sensors, suggesting its potential application for gaseous $H_2S$ sensing. Such an efficient on-site visual determination of gaseous hydrogen sulfide ($H_2S$) is highly demanded in on-site environmental monitoring and protection.

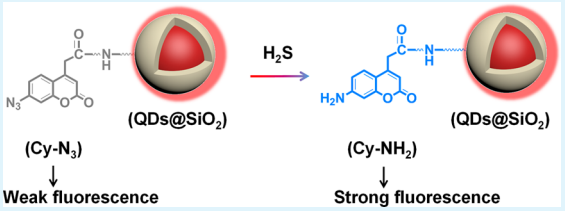


**KEYWORDS:** *functionalized quantum dots, quantum dots embedded silica nanoparticles, nanohybrid probe, azidocoumarin, hydrogen sulfide*

## INTRODUCTION

Recently, growing attention has been paid to semiconductor quantum dots because of their potential applications in micro/nano electronics, solar cells, and biolabeling and bioimaging.[1−3] In addition, QDs have superior spectroscopic properties including broad range of excitation wavelength, tunable maximum emission wavelength, symmetric and narrow fluorescence spectrum, and feasibility of the surface functionalization, which could make them excellent fluorophores for potential important applications, for example, as fluorescence probes.[4−8] The exploration of QDs' application in sensing and detection by manipulating their surface properties is very significant for advances of nanoscience and nanotechnology.[9,10] Generally, QDs are comprised of two parts: one is the inorganic nanocrystal core, such as CdTe, CdSe, or CdSe−ZnS, while the other is organic shells, such as mercaptoundecanoic acid (MUA) and 3-mercaptopropionic acid (MPA) for stabilization, which are linked through surface sulfide of the mercapto groups.[11] The surface sulfides are vulnerable to protonation at low pH condition, leading to fluorescence quenching due to generation of surface defects of QDs.[12] It was reported that the surface sulfide of mercapto-groups on QDs was easy to photo-oxidize and hydrolyze.[13,14] Thus, it has been proposed and demonstrated that the stability of QDs can be partially improved by wrapping them with inert silica ($SiO_2$) shells to resist photo-oxidation and hydrolysis.[15−18] We therefore anticipate that specific practical applications could be achieved by further functionalizing the surface of silica nanospheres, through a Si−O linker, with target functional molecules.

In this work, we first encapsulated MPA-CdTe QDs in silica shells and subsequently functionalized the silica surface with a functional molecule, azidocoumarin-4-acetic acid (Cy-$N_3$), to fabricate a novel ratiometric fluorescence nanohybrid probe. The nanohybrid probe shows two emission peaks, in which the red-colored fluorescence of QDs is inert to $H_2S$, whereas the weak blue-colored fluorescence of the Cy-$N_3$ is very responsive to $H_2S$ under mild conditions, which greatly enhances the fluorescence of the coumarin fluorophore.[19−22] Thus, the azido group in the nanohybrid probe can selectively recognize the molecule of $H_2S$, exhibiting good selectivity for the identification of $H_2S$. The different responses to $H_2S$ result in a distinct fluorescence color change from light magenta to blue. Thus, this method could be applied for the visualization of gaseous $H_2S$, which is a kind of colorless, water-soluble, highly

Received: October 22, 2014
Accepted: January 23, 2015
Published: January 23, 2015




DOI: 10.1021/am507307g
ACS Appl. Mater. Interfaces 2015, 7, 3547−3553

flammable, and poisonous gas at ambient temperatures and has attracted increasing concerns about environmental pollution. It can cause respiratory paralysis and rapidly fatigue the sense of smell at high concentrations, so smell cannot be depended on as a warning of exposure. It is also an important endogenous gasotransmitter and performs vital roles in many physiological processes,[23,24] including cardioprotection, neuromodulation, vasodilation, anti-inflammation, central nervous, respiratory, gastrointestinal, and endocrine systems.[25−31] Meanwhile, there is an equilibrium between $H_2S$ and $HS^-$ in aqueous solution, the predominant sulfide species under biological conditions, which has been correlated to arterial, pulmonary hypertension, Alzheimer's, and other diseases.[32,33] Therefore, sensitive and selective determination for hydrogen sulfide in aqueous media is very significant for both environment monitoring and human health.

Traditional approaches including metal-induced sulfide precipitation, colorimetric, electrochemical, and gas chromatography have been employed for the detection of trace $H_2S$.[34−38] Although these methods can meet the sensitivity requirements, the operation often requires tedious and strict sample preparation procedures. Recently, chemiresistive gas sensors based on thin films of metal oxides have been extensively explored for gaseous $H_2S$.[39,40] As compared to these methods, ratiometric fluorescence methods use two independent fluorescence signals: one is sensitive to hydrogen sulfide, and the other is inert and acts as an internal standard. Thus, the main advantage of the present method is the built-in correction for measuring conditions, such as probe concentration and excitation source power.[8,17,41−44] The ratiometric method also can achieve visualization of the analyte on the basis of fluorescence intensities ratios at two wavelengths, which are more favorable for practical applications (Supporting Information Table S1).[21,22,45−48]

Herein, we fabricate a novel nanohybrid probe by taking advantage of the superior fluorescence properties of nanomaterials. The fluorescent QDs were first encapsulated by growing silica shell on the surface. The silica shell was subsequently functionalized with functional amino groups by covalently bonding molecule 3-aminopropyltriethoxysilane on the surface. The functional molecules (azidocoumarin-4-acetic acids, Cy-$N_3$) were covalently linked to the silica nanosphere surface through a condensation reaction between the carboxyl groups of Cy-$N_3$ and the amino groups on the silica surface, to produce the final nanohybrid probe. The nanohybrid probe shows a good limit of detection as estimated to be 7.0 nM in aqueous medium. In addition, such a nanohybrid probe has also been applied for gaseous $H_2S$ determination with a good sensitivity and selectivity, implying its potential application for $H_2S$ detection.

## EXPERIMENTAL SECTION

**Materials.** Reduced glutathione (GSH), L-cysteine (L-Cys), 3-mercaptopropionic acid (MPA), mercaptoundecanoic acid (MUA), sodium azide ($NaN_3$), sodium sulfate ($Na_2SO_4$), sodium bisulfate ($NaHSO_4$), sodium sulfite ($Na_2SO_3$), sodium thiosulfate ($NaS_2O_3$), sodium sulfide ($Na_2S$), sodium thiocyanate (NaSCN), hydrogen peroxide ($H_2O_2$), *tert*-butylhydroperoxide (TBHP), sodium hypochlorite (NaClO), sodium nitrite ($NaNO_2$), sodium nitrate ($NaNO_3$), potassium superoxide ($KO_2$), tetraethylorthosilicate (TEOS), 3-mercaptopropyltrimethoxysilane (MPS), 3-aminopropyltriethoxysilane (APTS), 3-aminophenol, ethyl chloroformate, 1,3-acetonedicarboxylic acid, *N*-hydroxysuccinimide (NHS), and 1-(3-(dimethylamino)-propyl)-3-ethylcarbodiimide hydrochloride (EDC) were purchased from Sigma-Aldrich. Absolute ethanol, ethyl acetate (EtOAc), concentrated sulfuric acid ($H_2SO_4$), ammonium hydroxide (25%), and *N*,*N*-dimethyformamide (DMF) were received from Sinopharm Chemical Reagent Co., Ltd. (Shanghai, China). The PBS buffer was prepared with $Na_2HPO_4{\cdot}12H_2O$, $NaH_2PO_4{\cdot}2H_2O$, and NaCl solution.

**Apparatus.** Fluorescence spectra, Fourier transform infrared (FT-IR) spectra, and UV−vis absorption spectra were recorded by a PerkinElmer LS-55 luminescence spectrometer, Thermo Fisher Nicolet iS10 FT-IR spectrometer, and Shimadzu UV-2550 spectrometer, respectively. The transmission electron microscopy (TEM) images were recorded on a JEOL 2010 transmission electron microscope. Fluorescence photos were taken using a Canon 350D digital camera.

**Fabrication of Red Fluorescent QDs Stabilized in Silica Nanoparticles.** The hydrophilic red fluorescent CdTe quantum dots were prepared using an approach previously reported.[11] The red fluorescent QDs were then encapsulated in silica nanospheres by following a slightly modified Stöber method.[18,49] In a typical synthesis, 5 mL of red QDs was first added into a solvent mixture containing 15 mL of ultrapure water, 40 mL of ethanol, and 20 μL of MPS in a 100 mL flask. The mixture was then stirred for 6 h at room temperature. Next, 500 μL of TEOS and 500 μL of $NH_3{\cdot}H_2O$ were introduced into the mixture, followed by stirring for 12 h. Finally, to functionalize the silica surface with amino groups, 100 μL of APTS was injected to the above mixture solution and stirred for another 12 h. After the reaction, the as-prepared nanoparticles were alternately washed with ethanol and ultrapure water for three runs to remove the excess unreacted chemicals.

**Synthesis of 7-Azidocoumarin-4-acetic Acid (Cy-$N_3$).** 7-Aminocoumarin-4-acetic acid (Cy-$NH_2$) was prepared according to the literature.[50] Cy-$N_3$ was synthesized by diazotization of Cy-$NH_2$ followed by sodium azide displacement using a method adapted from the literature.[51,52] Briefly, 1.0 g of Cy-$NH_2$ was suspended in 22 mL of $H_2O$ cooled in an ice bath to keep the reaction at 0 °C. Next, 5.4 mL of sulfuric acid ($H_2SO_4$, 70%) was added slowly into the above solution in an ice bath. When the solution became homogeneous, 6.7 mL of $NaNO_2$ aqueous solution (0.82 M) was added dropwise over 30 min, followed by stirring for 1 h at 0 °C. After the reaction, 4 mL of $NaN_3$ solution (1.88 M) was introduced slowly into the mixture solution and stirred for further 12 h. The pure Cy-$N_3$ of dark-yellow was precipitated and filtered on a glass fritted funnel, then washed extensively with water and dried in vacuo to remove traces of water.

**Surface Functionalization of Quantum Dots Embedded in Silica Nanoparticles with Cy-$N_3$.** In a typical method, 24 mg of Cy-$N_3$ was dissolved in 1 mL of DMF and mixed with 1 mL of $H_2O$ to form a homogeneous solution in a 10 mL flask. To activate the carboxyl groups of Cy-$N_3$, 3 mL of EDC/NHS solution (2 mg/mL) was then injected into the above solution and stirred for 15 min. Ten milligrams of APTS-modified silica nanoparticles containing free surface amine groups was added into the above solution and was vigorously stirred for 6 h at room temperature in the dark. The resultant nanohybrid particles were precipitated through centrifugation and purified by washing three times with ultrapure water to remove unreacted reagents. The product of nanohybrid probe was dispersed in PBS (10 mM, pH 7.4) solution with a final concentration of 3.5 mg/mL for future use.

The analytical performance of the nanohybrid probe is related to the amount of Cy-$N_3$ loaded on the surface of CdTe@$SiO_2$. An optimal mass ratio of Cy-$N_3$ to CdTe@$SiO_2$ was found to be 2.4:1, resulting in broad color change from light magenta to blue (Supporting Information Figure S1A), indicating that more concentration levels of $H_2S$ can be determined by different colors. The fabrication of such nanohybrid can be easily repeated with a good reproducibility, as evidenced by three independent repetitions (Supporting Information Figure S1B). The other loading mass ratios with less or more Cy-$N_3$ on CdTe@$SiO_2$ only produced narrow color changes. For example, a mass ratio of 1:1 resulted in a change from red to pink (Supporting Information Figure S1C). When the mass ratio was increased to as high as 6:1, a small color change from violet to blue can be observed (Supporting Information Figure S1D).


DOI: 10.1021/am507307g
ACS Appl. Mater. Interfaces 2015, 7, 3547−3553

**Procedures for Sample Preparation and Fluorescence Experiments Using the Dual Emission Nanohybrid Probe.** The stock solutions of the reactive species (GSH, L-Cys, MPA, $NaHSO_4$, $NaS_2O_3$, $Na_2SO_4$, $Na_2SO_3$, NaSCN, $NaNO_2$, $NaNO_3$, TBHP) were prepared directly by dissolving them in ultrapure water to get the concentration of 1 mM, respectively. The ethanol solution of MUA (0.1 mM) was obtained by directly dissolving in ethanol. The concentrations of freshly prepared $H_2O_2$ (240 nm, $\varepsilon$ = 43.6 $M^{-1}$ $cm^{-1}$), $KO_2$ (550 nm, $\varepsilon$ = 21.6 $mM^{-1}$ $cm^{-1}$), peroxynitrite anion $ONOO^-$ (302 nm, $\varepsilon$ = 1670 $M^{-1}$ $cm^{-1}$), HClO (292 nm, $\varepsilon$ = 350 $M^{-1}$ $cm^{-1}$), and $SO_2$ (288 nm, $\varepsilon$ = 365 $M^{-1}$ $cm^{-1}$) were determined on the basis of their UV absorbances and extinction coefficients before use.[53−57] Nitrogen dioxide ($NO_2$) was estimated to be 1.4 mM by colorimetric method using ammonium 2,2′-azinobis(3-ethylbenz othiazoline-6-sulfonate) (ABTS) as an indicator.[58] Carbon monoxide (CO) gas was prepared by dropping slowly formic acid on concentrated sulfuric acid heated in a 100 mL flask.[59] $NH_3$ gas was prepared from the reaction of $NH_4Cl$ with $Ca(OH)_2$ in a 50 mL flask. $NO_2$ gas sample was prepared by diluting the pure $NO_2$ gas. $SO_2$ gas was prepared from the reaction of $NaHSO_3$ with concentrated $H_2SO_4$. $H_2S$ gas was prepared from the reaction of $Na_2S$ with $H_3PO_4$ in a 100 mL flask. These species were added into the nanohybrid probe (52 $\mu$g/mL) solution in PBS buffer (10 mM, 7.4). The fluorescence spectra of these systems were then recorded at 5, 10, and 15 min after adding each of these RSS/ROS species, respectively.

## RESULTS AND DISCUSSION

**Fluorescent Characteristics of the As-Prepared Nanohybrid Probe.** The structure of the nanohybrid probe and the principle for visual detection of $H_2S$ are presented in Scheme 1.

**Scheme 1. Schematic Illustrating the Structure of Nanohybrid Probe and the Principle for Detecting Hydrogen Sulfide, Which Is Based on $H_2S$ Reducing the Weak Blue Fluorescence Cy-$N_3$ to Strong Blue Fluorescence Cy-$NH_2$, while the Red Emission Stays Constant, Resulting in the Color Evolution from Light Magenta to Blue**

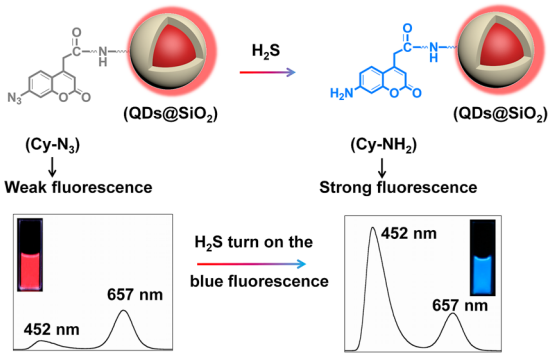


The Cy-$N_3$ component acts as a specific recognition site for $H_2S$ to produce strong blue fluorescent Cy-$NH_2$, while the QDs@$SiO_2$ component is stable against $H_2S$, resulting in variation of the fluorescence intensity ratio of the nanohybrid probe and apparent fluorescence color changes. To fabricate such a nanohybrid probe, the MPA-CdTe QDs (Supporting Information Figure S2a) were first wrapped with silica shell, followed by further surface functionalization with 3-aminopropyltriethoxysilane to get red fluorescent QDs@$SiO_2$ nanoparticles with end amino groups (Supporting Information Figure S2b). The surface amino group could readily react with the activated carboxyl group of the weakly fluorescent molecules (Cy-$N_3$, Supporting Information Figure S2c) catalyzed by EDC/NHS to generate the nanohybrid probe. Such nanohybrid probe can be easily dispersed in water and shows a light-magenta fluorescence under UV light illumination (Supporting Information Figure S2d).

The sizes and morphologies of QDs, QDs@$SiO_2$ nanoparticle, and the nanohybrid probe are respectively examined with TEM (Supporting Information Figure S3). Both the QDs@$SiO_2$ nanoparticle and the nanohybrid probe are well-dispersed and have similar average sizes of about 50 nm. The results show that the introducing of Cy-$N_3$ molecules to the surface of the silica shell did not change the size and morphology of the QDs-embedded silica nanoparticles. This is reasonable because the nanohybrid probes are prepared by covalently bonding a monolayer of small organic molecules on the surface of QDs@$SiO_2$ nanoparticle. The photostability of the nanohybrid probe has also been examined by 12 consecutive illuminations under UV light (5 min for each time). The results show that the two fluorescence intensity ratios of the nanohybrid probe remain almost constant (Supporting Information Figure S4), implying the probe's good photostability in aqueous solution.

**Response of Nanohybrid Probe to $H_2S$.** Figure 1 shows the fluorescence spectra of the nanohybrid probe upon the addition of sodium hydrosulfide in aqueous solution. Clearly, the blue emission gradually increased upon time after the addition of sodium hydrosulfide, which could be attributed to the production of strongly fluorescent Cy-$NH_2$ from the reduction of weakly fluorescent Cy-$N_3$ by hydrosulfide. Unlike the Cy-$N_3$ on the surface of the nanohybrid probe, the red fluorescence from QDs@$SiO_2$ remained constant. The different fluorescence responses of the two components of the nanohybrid probe to $H_2S$ resulted in a distinct fluorescence color change from light magenta to blue as the fluorescence intensity ratio increased, as shown in Figure 1A. The difference color responses clearly demonstrated the advantages of the nanohybrid probe for visual detection. As compared to pure blue Cy-$N_3$, the nanohybrid probe possesses three advantages. First, the nanohybrid probe results in distinct color grading, which is dependent on the amount of hydrogen sulfide. More detailed comparisons were performed to demonstrate the ratiometric probe is more easily visualized than a single color change of pure Cy-$N_3$ (Supporting Information Figure S5), which is hard to distinguish (Figure 1B). Second, it has an internal standard fluorescence of quantum dots, which can be used for quantification independent of the probe concentration. Third, the covalent bonding of Cy-$N_3$ on the surface of nanoparticles reduces the probability of its self-quenching, which can enhance the sensitivity.

**Reaction Mechanism of the Nanohybrid Probe with $H_2S$.** The blue fluorescence enhancement of the nanohybrid probe could be attributed to the reduction of Cy-$N_3$ to Cy-$NH_2$ by $H_2S$, which is based on the unique reaction between azido group and hydrogen sulfide.[16−19,36] We reason that the Cy-$N_3$ dye becomes caged by the azido, an electron-withdrawing group showing weak fluorescence (QY, 0.96%), which can be selectively reduced by $H_2S$ back to highly fluorescent Cy-$NH_2$ (QY, 76%, Supporting Information Figure S6) with an amino group. The reduction of Cy-$N_3$ by $H_2S$ could be evidenced by monitoring the change of IR spectra. First, the intense band at 2117 $cm^{-1}$ is a characteristic vibration of the azido group. It disappears after reaction with hydrogen sulfide, and the new intense band at 3475 $cm^{-1}$ appears, which is ascribed to N−H stretching of amino groups (Supporting Information Figure S7). The results prove the successful reduction of Cy-$N_3$ to Cy-


DOI: 10.1021/am507307g
ACS Appl. Mater. Interfaces 2015, 7, 3547−3553

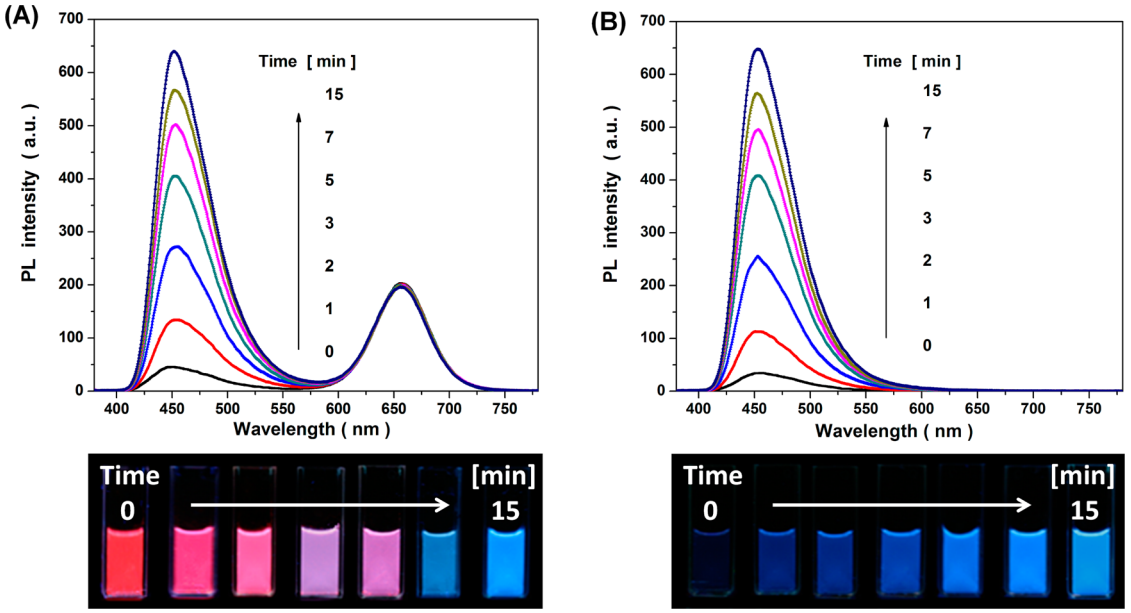


**Figure 1.** Fluorescence responses of (A) the nanohybrid probe and (B) the pure blue Cy-$N_3$ upon the addition of NaHS (2 $\mu$M) in PBS buffer solution (10 mM, pH 7.4). The fluorescence spectra were respectively collected at 1, 2, 3, 5, 7, and 15 min after the addition of 2 $\mu$M NaHS. Ex = 365 nm, filter 430 nm. The bottom images show the corresponding fluorescence photos taken under the illumination of a UV lamp.

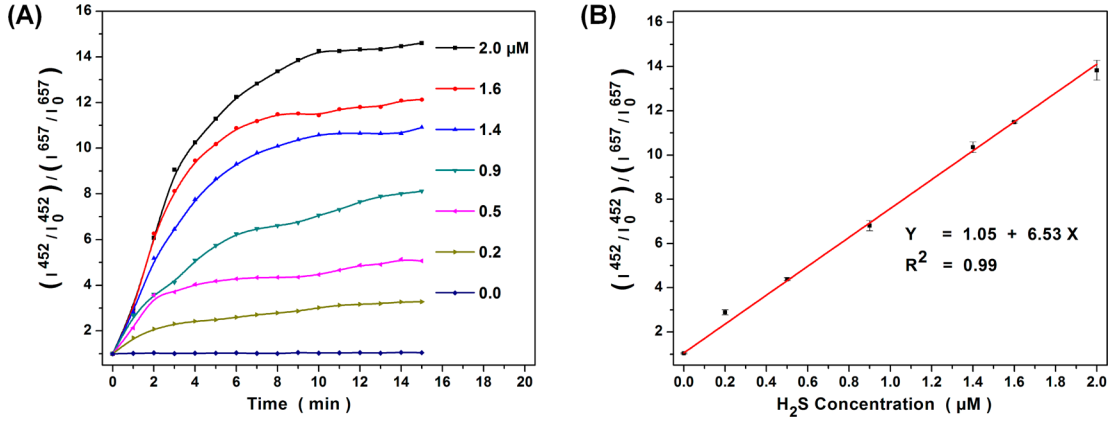


**Figure 2.** (A) The increment of fluorescence intensity ratio against reaction time (0−15 min) after adding different amounts of NaHS. (B) The plot of fluorescence intensity ratio versus the concentration of NaHS. $I_0^{452}$, $I^{452}$ and $I_0^{657}$, $I^{657}$ were the fluorescence intensities of nanohybrid probe at 452 and 657 nm before and after addition of NaHS, respectively. The fluorescence data were recorded at 10 min after adding NaHS.

$NH_2$ by $H_2S$. The other intense bands at 1733 and 1689 $cm^{-1}$ are assigned to the vibrations of C═O in the ester and carboxyl groups, respectively (Supporting Information Figure S7A). The band at 1170 and 1100 $cm^{-1}$ are due to the stretching of C−N vibrations and asymmetric stretch of C−O−C of Cy-$N_3$, respectively.[48] The vibration frequencies of the carbonyl group at 1655 $cm^{-1}$ and the C−N and C−O−C vibration stretch still remain after reduction by hydrogen sulfide.

**Kinetic Fluorescence Response to $H_2S$.** To evaluate the dose dependence and kinetics of the nanohybrid probe to $H_2S$, the fluorescence intensity ratios were monitored at different reaction times after the addition of various amounts of $H_2S$, as shown in Figure 2A. The fluorescence enhancement of the nanohybrid probe against the amount of $H_2S$ was plotted in Figure 2B. Clearly, the fluorescence intensity ratio can be linearly correlated to the concentration of $H_2S$ with a coefficient of 0.99. The limit detection (LOD) of the method was estimated to be 7.0 nM in aqueous solution according to the definition of 3 times the deviation of the blank signal ($3\sigma$). Furthermore, we investigated whether the linear relationship was maintained at different reaction times. The results showed that the linear relationship was obeyed well at reaction times longer than 2 min (Supporting Information Figure S8).

**Interference Study.** The relevant sulfur/oxygen species (GSH, L-Cys, MPA, MUA, $NaHSO_4$, $NaS_2O_3$, $Na_2SO_4$, $Na_2SO_3$, NaSCN, $NaNO_2$, $NaNO_3$, $H_2O_2$, TBHP, HClO, $KO_2$, $ONOO^-$, $NO_2$, $SO_2$, CO) were carefully studied to examine the selectivity for $H_2S$. Figure 3A demonstrated that the fluorescence intensity ratios are not affected much by other reactive sulfur/oxygen species (RSS/ROS, 20 $\mu$M) in the probe solution. It can be noted the fluorescence intensity ratios of $NO_2$, $SO_3^{2-}$, and CO are slightly different from other species at 15 min, but the fluorescence colors are similar in the photos. This could be due to the low color resolution of the digital camera used. Actually, the fluorescence differences of the three species from other species can be noted by the naked eye. Unlike these species, $H_2S$ greatly increases the fluorescence intensity ratio at a lower concentration of 2.0 $\mu$M (Figure 3B).


DOI: 10.1021/am507307g
ACS Appl. Mater. Interfaces 2015, 7, 3547−3553

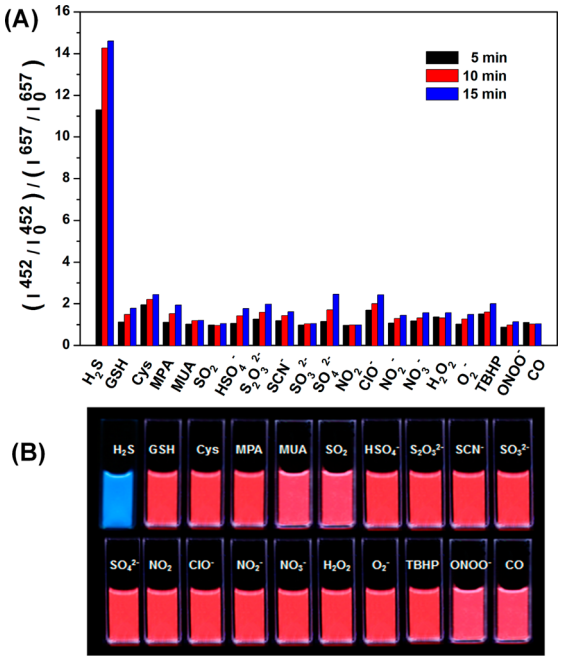


**Figure 3.** (A) Selectivity of the nanohybrid probe for $H_2S$ (2.0 $\mu$M). The graph was obtained at 5, 10, 15 min after adding other RSS/ROS species (20 $\mu$M). (B) Digital photos were taken under UV light 15 min after adding the species.

The results indicate that the nanohybrid probe possesses good selectivity for the identification of $H_2S$ among other RSS/ROS.

There is a fast conversation and equilibrium between $H_2S$ and $HS^-$ in aqueous medium. It is expected that the nanohybrid probe has also potential for the detection of gaseous $H_2S$ by simple and proper handling. The time course of nanohybrid probe to $H_2S$ gas was first conducted to show that the fluorescence intensity ratio of the probe was increased 20-fold in 15 min and remained almost unchanged (Supporting Information Figure S9). The result showed that it took 15 min to complete the reaction between $H_2S$ and the nanohybrid probe. To demonstrate the detection of gaseous $H_2S$, gas samples containing various concentrations of $H_2S$ were syringed slowly to the nanohybrid probe solution, followed by recording the fluorescence spectra at 15 min after the addition (Supporting Information Figure S10). The plot of fluorescence intensity ratio of the nanohybrid probe against the concentration of gaseous $H_2S$ showed a good linear relationship ($R^2$ = 0.988, Supporting Information Figure S10B), which can be used for the quantification of gaseous $H_2S$.

The selectivity of the method for various possible gases was also conducted for $CO_2$, $NO_2$, CO, $SO_2$, and $NH_3$. The experiments were carried out by following the same procedure as $H_2S$. The results show that no significant fluorescence intensity ratio changes of the nanohybrid probe were obtained after exposure to these gas samples, indicating a good selectivity for the identification of gaseous $H_2S$ as shown in Supporting Information Figure S11.

**Portable Gas Sensor for Visual Detection of Gaseous $H_2S$.** This nanohybrid probe also works well for the detection of gaseous hydrogen sulfide, a highly toxic gas in the atmosphere. For this purpose, the nanohybrid probe solution (2 $\mu$L) was first dropped onto a piece of glass-sheet to form indicating spots about 5 mm in diameter after air-drying. The gaseous $H_2S$ indicator spots were first exposed to gas samples containing different amounts of $H_2S$ gas for 5, 10, and 15 min. These indicating spots were then illuminated under a UV lamp, and the fluorescence images were taken (Figure 4). Clearly, the

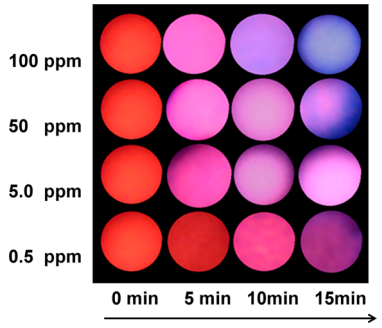


**Figure 4.** Visual detection of gaseous $H_2S$. The concentrations of $H_2S$ from bottom to top are 0.5, 5, 50, and 100 ppm, respectively. The fluorescence images were taken at 0, 5, 10, and 15 min after exposure to $H_2S$ gas under UV lamp, respectively.

method can detect gaseous $H_2S$ with a low concentration of 0.5 ppm, and 5 min exposure is enough for the sensor to develop distinct fluorescence colors (lavender pink) for $H_2S$ at 5.0 and 50 ppm levels. Thus, for gaseous hydrogen sulfide samples, the short-term and long-term detection limits of $H_2S$ are estimated to be 5 and 0.5 ppm, which could be noted when compared to the fluorescence color before exposure to $H_2S$ samples (Figure 4). The American Conference of Governmental Industrial Hygienists (ACGIH) short-term exposure limit (STEL) is 15 ppm for $H_2S$, and a single exposure period should not exceed 15 min. Furthermore, the United States Occupational Safety and Health Administration (OSHA) dose specifies a single 10 min exposure not to exceed 50 ppm. Therefore, the $H_2S$ indicator can be used as a simple, rapid, and portable sensor for monitoring the contamination of gaseous $H_2S$.

## CONCLUSION

We designed a fluorescence nanohybrid probe, and the probe demonstrated its good performance for on-site visual determination of $H_2S$. Such a nanohybrid probe was obtained by first encapsulating inorganic MPA-CdTe QDs in silica shells and then modifying the silica surface with functional organic molecules Cy-$N_3$, which act as the specific reaction site for $H_2S$. Under the excitation of a single light source, the nanohybrid probe exhibits two emissions at 452 and 657 nm, respectively. The red fluorescence was inert to $H_2S$, whereas the blue fluorescence could be selectively enhanced by $H_2S$, resulting in continuous fluorescence color changes from light magenta to blue. The detection limit of this method was 7.0 nM in aqueous solution. In addition, the method can detect gaseous $H_2S$ with a low concentration of 0.5 ppm by the indicator sensor, which can be used for the determination of $H_2S$ content in gas samples.

## ASSOCIATED CONTENT

### Supporting Information

Comparison of results with other methods, the synthetic routes for Cy-$N_3$ and nanohybrid probe, the TEM of QDs, QDs@$SiO_2$ and nanohybrid probe, the stability of nanohybrid probe, the QY and IR of Cy-$N_3$ before and after addition of $H_2S$, the response of nanohybrid probe to gaseous $H_2S$, and its


DOI: 10.1021/am507307g
ACS Appl. Mater. Interfaces 2015, 7, 3547−3553

selectivity for other gas species. This material is available free of charge via the Internet at http://pubs.acs.org.

## AUTHOR INFORMATION


### Corresponding Author

*Phone: 86-551-65591812. Fax: 86-551-65591156. E-mail: shwang@iim.ac.cn.

### Author Contributions

‖Y.Y. and H.Y. contributed equally.


### Notes

The authors declare no competing financial interest.

## ACKNOWLEDGMENTS

We thank the National Basic Research Program of China (2011CB933700) and the National Natural Science Foundation of China for grants (nos. 21205120, 21228702, 21475134).

## REFERENCES


(1) Zrazhevskiy, P.; True, L. D.; Gao, X. H. Multicolor Multicycle Molecular Profiling with Quantum Dots for Single-cell Analysis. *Nat. Protoc.* **2013**, *8*, 1852−1869.

(2) Gaponik, N. P.; Talapin, D. V.; Rogach, A. L.; Eychmüller, A. Electrochemical Synthesis of CdTe Nanocrystal/Polypyrrole Composites for Optoelectronic Applications. *J. Mater. Chem.* **2000**, *10*, 2163−2166.

(3) Somers, R. C.; Bawendi, M. G.; Nocera, D. G. CdSe Nanocrystal Based Chem-/Bio- Sensors. *Chem. Soc. Rev.* **2007**, *36*, 579−591.

(4) Liu, W. H.; Chio, H. S.; John, P. Z.; Eiichi, T.; Frangioni, J. F.; Bawendi, M. Compact Cysteine-Coated CdSe(ZnCdS) Quantum Dots for in Vivo Applications. *J. Am. Chem. Soc.* **2007**, *129*, 14530−14531.

(5) Mattoussi, H.; Palui, G.; Na, H. B. Luminescent Quantum Dots as Platforms for Probing in Vitro and in Vivo Biological Processes. *Adv. Drug Delivery Rev.* **2012**, *64*, 138−166.

(6) Cao, H. Q.; Wang, G. Z.; Zhang, S. C.; Zhang, X. R.; Rabinovich, D. Growth and Optical Properties of Wurtzite-Type CdS Nanocrystals. *Inorg. Chem.* **2006**, *45*, 5103−5108.

(7) Sun, J.; Yan, Y. H.; Sun, M. T.; Yu, H.; Zhang, K.; Huang, D. J.; Wang, S. H. Fluorescence Turn-On Detection of Gaseous Nitric Oxide Using Ferric Dithiocarbamate Complex Functionalized Quantum Dots. *Anal. Chem.* **2014**, *86*, 5628−5632.

(8) Zhu, H. J.; Zhang, W.; Zhang, K.; Wang, S. H. Dual-Emission of a Fluorescent Graphene Oxide−Quantum Dot Nanohybrid for Sensitive and Selective Visual Sensor Applications Based on Ratiometric Fluorescence. *Nanotechnology* **2012**, *23*, 315502.

(9) Das, B. C.; Pal, A. J. Core Shell Hybrid Nanoparticles with Functionalized Quantum Dots and Ionic Dyes: Growth, Monolayer Formation, and Electrical Bistability. *ACS Nano* **2008**, *2*, 1930−1938.

(10) Dorokhin, D.; Hsu, S. H.; Tomczak, N.; Reinhoudt, D. N.; Huskens, J.; Velders, A. H.; Vancso, G. J. Fabrication and Luminescence of Designer Surface Patterns with-Cyclodextrin Functionalized Quantum Dots via Multivalent Supramolecular Coupling. *ACS Nano* **2010**, *4*, 137−142.

(11) Zhang, K.; Mei, Q. S.; Guan, G. J.; Liu, B. H.; Wang, S. H.; Zhang, Z. P. Ligand Replacement-Induced Fluorescence Switch of Quantum Dots for Ultrasensitive Detection of Organophosphorothioate Pesticides. *Anal. Chem.* **2010**, *82*, 9579−9586.

(12) Wang, S. H.; Song, H. P.; Ong, W. Y.; Han, M. Y.; Huang, D. J. Positively Charged and pH Self-Buffering Quantum Dots for Efficient Cellular Uptake by Charge Mediation and Monitoring Cell Membrane Permeability. *Nanotechnology* **2009**, *20*, 425102.

(13) Liu, Y. S.; Sun, Y. H.; Vernier, P. T.; Liang, C. H.; Chong, S. Y.; Gundersen, M. A. pH-sSensitive Photoluminescence of CdSe/ZnSe/ZnS Quantum Dots in Human Ovarian Cancer Cells. *J. Phys. Chem. C* **2007**, *111*, 2872−2878.

(14) Sun, Y. H.; Liu, Y. S.; Vernier, P. T.; Liang, C. H.; Chong, S. Y.; Marcu, L.; Gundersen, M. A. Photostability and pH Sensitivity of CdSe/ZnSe/ZnS Quantum Dots in Living Cells. *Nanotechnology* **2006**, *17*, 4469−4476.

(15) Folling, J.; Polyakova, S.; Belov, V.; Blaadern, A. V.; Bossi, M. L.; Hell, S. F. Synthesis and Characterization of Photoswitchable Fluorescent Silica Nanoparticles. *Small* **2008**, *4*, 134−142.

(16) Li, H. B.; Qu, F. G. Synthesis of CdTe Quantum Dots in Sol-gel-derived Composite Silica Spheres Coated with Calix[4]arene as Luminescent Probes for Pesticide. *Chem. Mater.* **2007**, *19*, 4148−4154.

(17) Zhang, K.; Zhou, H. B.; Mei, Q. S.; Wang, S. H.; Guan, G. J.; Liu, R. Y.; Zhang, J.; Zhang, Z. P. Instant Visual Detection of Trinitrotoluene Particulates on Various Surfaces by Ratiometric Fluorescence of Dual-Emission Quantum Dots Hybrid. *J. Am. Chem. Soc.* **2011**, *133*, 8424−8427.

(18) Stöber, W.; Fink, A.; Bohn, E. Controlled Growth of Monodisperse Silica Spheres in the Micron Size Range. *J. Colloid Interface Sci.* **1968**, *26*, 62−69.

(19) Xuan, W. M.; Sheng, C. Q.; Cao, Y. T.; He, W. H.; Wang, W. Fluorescent Probes for the Detection of Hydrogen Sulfide in Biological Systems. *Angew. Chem., Int. Ed.* **2012**, *51*, 2282−2284.

(20) Kazemi, F.; Kiasat, A. R.; Sayyahi, S. Chemoselective Reduction of Azides with Sodium Sulfide Hydrate under Solvent Free Condition. *Phosphorus, Sulfur Silicon* **2004**, *179*, 1813−1817.

(21) Peng, H. J.; Cheng, Y. F.; Dai, C. F.; King, A. L.; Predmore, B. L.; Lefer, D. J.; Wang, B. H. A Fluorescent Probe for Fast and Quantitative Detection of Hydrogen Sulfide in Blood. *Angew. Chem., Int. Ed.* **2011**, *50*, 9672−9675.

(22) Lippert, A. R.; New, E. J.; Chang, C. J. Reaction-Based Fluorescent Probes for Selective Imaging of Hydrogen Sulfide in Living Cells. *J. Am. Chem. Soc.* **2011**, *133*, 10078−10080.

(23) E. Culotta, E.; Koshland, D. E. NO News is Good News. *Science* **1992**, *258*, 1862−1865.

(24) Morita, T.; Perrella, M. A.; Lee, M. E.; Kourembanas, S. Smooth Muscle Cell-derived Carbon Monoxide is a Regulator of Vascular cGMP. *Proc. Natl. Acad. Sci. U.S.A.* **1995**, *92*, 1475−1479.

(25) Miao, C. Y.; Li, Z. Y. The Role of Perivascular Adipose Tissue in Vascular Smooth Muscle cell Growth. *Br. J. Pharmacol.* **2012**, *165*, 643−658.

(26) Yang, G. D.; Wu, L. Y.; Jiang, B.; Yang, W.; Qi, J. S.; Cao, K.; Meng, Q. H.; Mustafa, A. K.; Mu, W. T.; Zhang, S. M.; Snyder, S. H.; Wang, R. $H_2S$ as a Physiologic Vasorelaxant: Hypertension in Mice with Deletion of Cystathionine g-Lyase. *Science* **2008**, *322*, 587−590.

(27) Li, L.; Bhatia, M.; Zhu, Y. Z.; Zhu, Y. C.; Ramnath, R. D.; Wang, Z. J.; Anuar, F. B.; Whiteman, M.; Salto-Tellez, M.; Moore, P. K. Hydrogen Sulfide is a Novel Mediator of Lipopolysaccharide-Induced Inflammation in the Mouse. *FASEB J.* **2005**, *19*, 1196−1198.

(28) Abe, K.; Kimura, H. The Possible Role of Hydrogen Sulfide as an Endogenous Neuromodulator. *J. Neurosci.* **1996**, *16*, 1066−1071.

(29) Boehning, D.; Snyder, S. H. Novel Neural Modulators. *Annu. Rev. Neurosci.* **2003**, *26*, 105−131.

(30) Kimura, H. Hydrogen Sulfide As a Neuromodulator. *Mol. Neurobiol.* **2002**, *26*, 13−19.

(31) Martelli, A.; Testai, L.; Breschi, M. C.; Blandizzi, C.; Virdis, A.; Teddei, S.; Calderone, V. Hydrogen Sulphide: Novel Opportunity for Drug Discovery. *Med. Res. Rev.* **2012**, *32*, 1093−1130.

(32) Li, L.; Rose, P.; Moore, P. K. Hydrogen Sulfide and Cell Signaling. *Annu. Rev. Pharmacol.* **2011**, *51*, 169−187.

(33) Szabo, C. Hydrogen Sulphide and Its Therapeutic Potential. *Nat. Rev. Drug Discovery* **2007**, *6*, 917−935.

(34) Hughes, M. N.; Centelles, M. N.; Moore, K. P. Making and Working with Hydrogen Sulfide the Chemistry and Generation of Hydrogen Sulfide in Vitro and Its Measurement in Vivo: A Review. *Free Radical Biol. Med.* **2009**, *47*, 1346−1353.

(35) Searcy, D. G.; Peterson, M. A. Hydrogen Sulfide Consumpt Ion Measured at Low Steady State Concentrations Using a Sulfidostat. *Anal. Biochem.* **2004**, *324*, 269−275.

(36) Lawrence, N. S.; Davis, J.; Jiang, L.; Jones, T. G. J.; Davies, S. N.; Compton, R. G. The Electrocheical Analog of the Methylene Blue




DOI: 10.1021/am507307g
ACS Appl. Mater. Interfaces 2015, 7, 3547−3553

Reaction: A Novel Amperometric Approach to the Detection of Hydrogen Sulfide. *Electroanalysis* **2000**, *18*, 1453−1460.
(37) Bérubé, P. R.; Parkinson, P. D.; Hall, E. R. Measurement of Reduced Sulphur Compounds Contained in Aqueous Matrices by Direct Injection into a Gas Chromatograph with a Flame Photometric Detector. *J. Chromatogr., A* **1999**, *830*, 485−489.
(38) Ishigami, M.; Hiraki, K.; Umemura, K.; Ogasawara, Y.; Ishii, K.; Kimura, H. A Source of Hydrogen Sulfide and a Mechanism of Its Release in The Brain. *Antioxid. Redox Signaling* **2009**, *11*, 205−214.
(39) Zhang, S. M.; Zhang, P. P.; Wang, Y.; Ma, Y. Y.; Zhong, J.; Sun, X. H. Facile Fabrication of a Well-Ordered Porous Cu-Doped $SnO_2$ Thin Film for $H_2S$ Sensing. *ACS Appl. Mater. Interfaces* **2014**, *6*, 14975−14980.
(40) Kaur, M.; Ramgir, N. S.; Gautam, U. K.; Ganapathi, S. K.; Bhattachaya, S.; Datta, N.; Saxena, V.; Debnath, A. K.; Aswal, D. K.; Gupta, S. K. $H_2S$ Sensors Based on $SnO_2$ Films: RGTO Verses RF Sputtering. *Mater. Chem. Phys.* **2014**, *147*, 707−714.
(41) Yu, Z. Q.; Kabashima, T.; Tang, C. H.; Shibata, T.; Kitazato, K.; Kobayashi, N.; Lee, M. K.; Kai, M. Selective and facile Assay of Human Immunodeficiency Virus Protease Activity by a Novel Fluorogenic Reaction. *Anal. Biochem.* **2010**, *397*, 197−201.
(42) Kabashima, T.; Yu, Z. Q.; Tang, C. H.; Nakagawa, Y.; Okumura, K.; Shibata, T.; Lu, J. Z.; Kai, M. A Selective Fluorescence Reaction for Peptides and Chromatographic Analysis. *Peptides* **2008**, *29*, 356−363.
(43) Hou, F. P.; Huang, L.; Xi, P. X.; Cheng, J.; Zhao, X. F.; Xie, G. Q.; Shi, Y. J.; Cheng, F. J.; Yao, X. J.; Bai, D. C.; Zeng, Z. Z. A Retrievable and Highly Selective Fluorescent Probe for Monitoring Sulfide and Imaging in Living Cells. *Inorg. Chem.* **2012**, *51*, 2454−2460.
(44) Montoya, L. A.; Pluth, M. D. Selective Turn-on Fluorescent Probes for Imaging Hydrogen Sulfide in Living Cells. *Chem. Commun.* **2012**, *48*, 4767−4769.
(45) Yu, F. B.; Li, P.; Song, P.; Wang, B. S.; Zhao, J. Z.; Han, K. L. An ICT-Based Strategy to a Colorimetric and Ratiometric Fluorescence Probe for Hydrogen Sulfide in Living Cells. *Chem. Commun.* **2012**, *48*, 2852−2854.
(46) Chen, B. F.; Li, W.; Lv, C.; Zhao, M. M.; Jin, H.; Jin, H. F.; Du, J. B.; Zhang, L. R.; Tan, X. J. Fluorescent Probe for Highly Selective and Sensitive Detection of Hydrogen Sulfide in Living Cells and Cardiac Tissues. *Analyst* **2013**, *138*, 946−951.
(47) Sasakura, K.; Hanaoka, K.; Shibuya, N.; Mikami, Y.; Kimura, Y.; Komatsu, T.; Ueno, T.; Terai, T.; Kimura, H.; Nagano, T. Development of A Highly Selective Fluorescence Probe for Hydrogen Sulfide. *J. Am. Chem. Soc.* **2011**, *133*, 18003−18005.
(48) Yu, C. M.; Li, X. Z.; Zeng, F.; Zheng, F. Y.; Wu, S. Z. Carbon-Dot-Based Ratiometric Fluorescent Sensor for Detecting Hydrogen Sulfide in Aqueous Media and Inside Live Cells. *Chem. Commun.* **2013**, *49*, 403−405.
(49) Yao, J. L.; Zhang, K.; Zhu, H. J.; Ma, F.; Sun, M. T.; Yu, H.; Sun, J.; Wang, S. H. Efficient Ratiometric Fluorescence Probe Based on Dual-Emission Quantum Dots Hybrid for On-Site Determination of Copper Ions. *Anal. Chem.* **2013**, *85*, 6461−6468.
(50) Maly, D. J.; Leonetti, F.; Backes, B. J.; Dauber, D. S.; Harris, J. L.; Craik, C. S.; Ellman, J. A. Expedient Solid-Phase Synthesis of Fluorogenic Protease Substrates Using the 7-Amino-4-Carbamoylmethylcoumarin (ACC) Fluorophore. *J. Org. Chem.* **2002**, *67*, 910−915.
(51) Kanaoka, Y.; Kobayashi, A.; Sato, E.; Nakayama, H.; Ueno, T.; Muno, D.; Sekine, T. Multifunctional Cross-Linking Reagents. I. Synthesis and Properties of Novel Photoactivable, Thio-Directed Fluorescent Reagents. *Chem. Pharm. Bull.* **1984**, *32*, 3926−3933.
(52) Zbigniew, L. P.; Winssinge, N. Fluorescence-Based Detection of Single Nucleotide Permutation in DNA via Catalytically Templated Reaction. *Chem. Commun.* **2007**, 3820−3822.
(53) Abo, M.; Urano, Y.; Hanaoka, K.; Terai, T.; Komatsu, T.; Nagano, T. Development of a Highly Sensitive Fluorescence Probe for Hydrogen Peroxide. *J. Am. Chem. Soc.* **2011**, *133*, 10629−10637.
(54) Izumi, S.; Urano, Y.; Hanaoka, K.; Terai, T.; Nagano, T. A Simple and Effective Strategy To Increase the Sensitivity of Fluorescence Probes in Living Cells. *J. Am. Chem. Soc.* **2009**, *131*, 10189−10200.
(55) Beckman, J. S.; Beckman, T. W.; Chen, J.; Marshall, P. A.; Freeman, B. A. Apparent Hydroxyl Radical Production by Peroxynitrite: Implicationsfor Endothelial Injury from Nitric Oxide and Superoxide. *Proc. Natl. Acad. Sci. U.S.A.* **1990**, *87*, 1620−1624.
(56) Sun, M. T.; Yu, H.; Zhu, H. J.; Ma, F.; Zhang, S.; Huang, D. J.; Wang, S. H. Oxidative Cleavage-Based Near-Infrared Fluorescent Probe for Hypochlorous Acid Detection and Myeloperoxidase Activity Evaluation. *Anal. Chem.* **2014**, *86*, 671−677.
(57) Leontiev, A. V.; Rudkevich, D. M. Revisiting Noncovalent $SO_2$-Amine Chemistry: An Indicator-Displacement Assay for Colorimetric Detection of $SO_2$. *J. Am. Chem. Soc.* **2005**, *127*, 14126−14127.
(58) Nims, R. W.; Cook, J. C.; Krishna, M. C.; Christodoulou, D.; P oore, C. M. B.; Miles, A. M.; Grisham, M. B.; Wink, D. A. Colorimetric Assays for Nitric Oxide and Nitrogen Oxide Species Formed from Nitric Oxide Stock Solutions and Donor Compounds. *Methods Enzymol.* **1996**, *268*, 93−105.
(59) Nudelman, N. S.; Doctorovich, F. Electro Transfer in The Reactions of Aryllithium Compounds with Carbon Monoxide. *Tetrahedron* **1994**, *50*, 4651−4666.


DOI: 10.1021/am507307g
*ACS Appl. Mater. Interfaces* 2015, 7, 3547−3553